REAL-TIME IMAGE DEMOIRÉING ON MOBILE DEVICES

Anonymous authors
Paper under double-blind review

ABSTRACT

Moiré patterns appear frequently when taking photos of digital screens, drastically degrading the image quality. Despite the advance of CNNs in image demoiréing, existing networks are with heavy design, causing massive computation burden for mobile devices. In this paper, we launch the first study on accelerating demoiréing networks and propose a dynamic demoiréing acceleration method (DDA) towards a real-time deployment on mobile devices. Our stimulus stems from a simple-yet-universal fact that moiré patterns often unbalancedly distribute across an image. Consequently, excessive computation is wasted upon non-moiré areas. Therefore, we reallocate computation costs in proportion to the complexity of image patches. In order to achieve this aim, we measure the complexity of an image patch by designing a novel moiré prior that considers both colorfulness and frequency information of moiré patterns. Then, we restore higher-complex image patches using larger networks and the lower-complex ones are assigned with smaller networks to relieve the computation burden. At last, we train all networks in a parameter-shared supernet paradigm to avoid additional parameter burden. Extensive experiments on several benchmarks demonstrate the efficacy of our proposed DDA. In addition, the acceleration evaluated on the VIVO X80 Pro smartphone equipped with a chip of Snapdragon 8 Gen 1 shows that our method can drastically reduce the inference time, leading to a real-time image demoiréing on mobile devices.

1 INTRODUCTION

Moiré patterns (Sun et al., 2018; Yang et al., 2017b) describe an artifact of images that in particular appears in television and digital photography. In contemporary society, using mobile phones to take screen pictures has become one of the most productive way to record information quickly. Nevertheless, moiré patterns occur frequently from the interference between the color filter array (CFA) of camera and high-frequency repetitive signal. The resulting stripes of different colors and frequencies on the captured photos drastically degrades the visual quality. Therefore, developing demoiréing algorithms has received long-time attention in the research community, and yet remains unsolved in particular when running algorithms on offline mobile devices.

Primitive studies on image demoiréing resort to traditional machine learning techniques such as low-rank and sparse matrix decomposition (Liu et al., 2015) and bandpass filters (Yang et al., 2017a). The rising of convolutional neural networks (CNNs) has vastly boosted the efficacy of image demoiréing (He et al., 2019; Zheng et al., 2020). However, the improved quantitative performance, such as PSNR (Peak Signal-to-Noise Ratio), comes at the increasing costs of energy and computation. For example, MBCNN (Zheng et al., 2020) eats up 4.22T floating-point operations (FLOPs) in order to restore a 1920×1080 smartphone-taken moiré image. Given that the moiré patterns mostly emerge in mobile photography, such massive computations considerably barricade the application of demoiréing networks on mobile devices. Therefore, it is of great need to bridge the technology gap between academia and industry.

To tackle the aforementioned issue, we initiate the first study on accelerating demoiréing networks towards a real-time deployment on mobile devices. Our motivation arises from empirical actuality in moiré images. As shown in Fig. 1, an image is often partially contaminated by the moiré. Some areas are filled with intensive moiré stripes, some are much relieved while some are kept away from moiré pollution. It is natural to hand out computation to these moiré centralized areas but less to

Figure 1: Images with moiré patterns. The blue boxes show a zooming-in area. Two phenomena can be observed: (1) The moiré complexity varies significantly across different areas of an image. (2) Moiré patterns are mainly characterized by frequency and colorfulness.

these diluted areas. In the extreme case, it is needless to cleanse uninfluenced areas. Unfortunately, existing methods Sun et al. (2018); Zheng et al. (2021) have not distinguished the treatment to the different areas in an image. They not only waste excessive computation on non-moiré areas but also bring about side effect, such as over-whitened image contents. Therefore, reallocating computation costs in compliance with the complexity of a moiré area can be a potential solution to accomplish real-time image demoiréing on mobile devices.

Stimulated by the above analysis, we opt to split a whole image into several sub-image patches. To measure the patch moiré complexity, we introduce a novel moiré prior. As can be referred in Fig. 1, moiré patterns are featured with either high frequency or rich color information. Thus, we define the moiré prior as the product of frequency and color information in a patch. Detailedly, we model the frequency information by a Gaussian filter and the colorfulness metric is a linear combination of the mean and standard deviation of the pixel cloud in the color plane of CIELab (Hasler & Suesstrunk, 2003). Using this prior to measure the moiré complexity, each image patch is then processed by a unique network with its computation costs in proportion to the moiré complexity. In this fashion, larger networks are utilized to restore moiré centralized areas to ensure the recovery quality while smaller networks are leveraged to restore moiré diluted areas to relieve computation burden. Consequently, we lead to a better tradeoff between the image quality and resource requirement on mobile devices.

Nevertheless, multiple networks lead to more parameter burden, which also causes deployment pressure due to the short-supply memory on mobile devices. To mitigate this issue, we leverage the supernet paradigm (Yang et al., 2021) to jointly train all networks in a parameter-shared manner. Concretely, we regard the vanilla demoiréing network as a supernet, and weight-shared subnets of different sizes are directly extracted from this supernet to process image patches of different demoiré complexity. During the training phase, each subnet is dynamically trained using corresponding image patches with similar moiré complexity. Consequently, the overall running overhead can be effectively reduced without introduction of any additional parameters.

We have conducted extensive experiments for accelerating existing demoiréing networks on the LCDMoiré (Yuan et al., 2019) and FHDMi (He et al., 2020) benchmarks. The results show that our dynamic demoiréing acceleration method, termed DDA, achieves an obviously FLOPs reduction even with PSNR and SSIM increases. For instance, DDA reduces 45.2% FLOPs of the state-of-the-art demoiréing network MBCNN Zheng et al. (2021) with 0.35 dB PNSR increase. Furthermore, the accelerated DMCNN Huang et al. (2017) leads to real-time image demoiréing on the VIVO X80 Pro smartphone, with a tiny latency of 48.0 ms when processing an image of 1920×1080 resolution.

This work addresses the problem of demoiréing network deployment on resource-hungry mobile devices. The key contributions of this paper include: (1) A novel framework for accelerating image demoiréing networks in a dynamic manner. (2) An effective moiré prior to identify the demoiréing complexity of a given image patch. (3) Performance maintenance and apparent acceleration on modern smartphones.

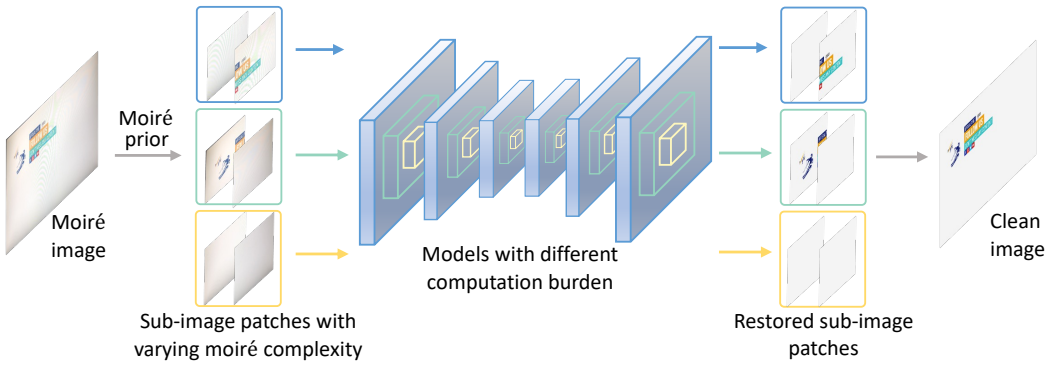

Figure 2: The framework of our proposed dynamic demoiréing acceleration method (DDA).

2 Related Work

2.1 Image Demoiréing

Image demoiréing aims at removing moiré patterns on captured images. Early work mainly focuses on manually designed algorithms with the aid of low-rank & sparse matrix decomposition (Yang et al., 2017a; Liu et al., 2015). With the explosion and popularity of deep learning, extensive demoiréing networks are proposed in recent years to achieve moiré removal in an end-to-end manner (Sun et al., 2018; He et al., 2019). As a pioneer work, (Sun et al., 2018) proposed a multi-scale network structure to remove moiré patterns at different frequencies and scales. (He et al., 2019) dived into designing specific learning schemes to resolve the unique properties of moiré patterns including frequency distributions, edge information and appearance attributes. (Zheng et al., 2020) reformulated the image demoiréing problem as moiré texture removal and color restoration, and proposed MBCNN (Zheng et al., 2020) which consists of a learnable bandpass filter to learn the frequency prior and a two-step tone mapping mechanism to restore color information. FHDe2Net (He et al., 2020) uses a global branch to eradicate multi-scale moiré patterns and a local branch to reserve fine details. (Liu et al., 2020) further proposed WavleNet to handle demoiréing in the wavelet domain. The same dilemma for the aforementioned networks is their huge computation burden, which greatly prohibits the practical deployment on mobile devices.

2.2 Dynamic Networks and Supernets

Dynamic networks adapt the network structures or parameters *w.r.t.* different inputs (Kong et al., 2021; Huang et al., 2017; Bolukbasi et al., 2017). Due to the advantages in accuracy performance and computation efficiency, dynamic networks have received increasing research interest in recent years. A comprehensive overview of dynamic networks can be found at (Han et al., 2021). Supernets are a type of dynamic network that reserves weight-shared sub-networks of multiple sizes in one network, and randomly samples these sub-networks for training (Chen et al., 2022; Yang et al., 2021; Yu & Huang, 2019). According to the resource constraints, different sub-networks with varying widths and resolutions can be chosen during the testing phase without additional parameter burden. Inspired by these studies, our proposed DDA involves the supernet paradigm by dynamically allocating image patches with different demoiréing complexity to their corresponding sub-networks.

3 Methodology

The general framework of our proposed dynamic demoiréing acceleration method (DDA) is manifested in Fig. 2. A moiré image is firstly split into several sub-image patches, which are then reorganized into different groups in conformity with the patch moiré complexity. This is achieved by a novel moiré prior that considers both color and frequency information of moiré patterns. We detail it in Sec. 3.1. For the purpose of real-time image demoiréing on mobile devices, we train

Figure 3: The sorted sub-image patches according to moiré complexity scores given by our proposed moiré prior.

multiple networks of different complexity to process patches in different groups. In the training and testing phases, higher-complex image patches are fed to larger networks and lower-complex ones are dealt with smaller networks. Sec. 3.2 gives the implementations. Finally, as an alternative for training separate networks that result in more parameters, we regard each one as a subnet of the vanilla demoiréing network (supernet), leading to a weight-shared training paradigm as depicted in Sec. 3.3.

3.1 Moiré Prior

The complexity degree of moiré patterns can be determined by human, however, it is lavish and laborious to manually define the complexity for all patches in every single one of the moiré image. Many former works on dynamic networks (Han et al., 2021; Kong et al., 2021) choose to train an additional module to adapt the network *w.r.t.* different inputs, which however, brings unexpected parameters and computations for its compositions of several convolutional or full-connected layers. Given our plan of deploying demoiréing networks on mobile devices, such a solution is not feasible, or at least not the optimal.

To solve this problem, we propose a novel moiré prior, which opens a new road to measure the moiré complexity of a given moiré image in a fast manner. The motivation for this prior comes from an in-depth observation on moiré images. As can be inferred from Fig. 3, moiré patterns vary a lot in frequency and colorfulness. Customarily, a perceptible moiré pattern is highlighted by either high frequency or rich color information. Therefore, a prior reflecting both image frequency and colorfulness can be an efficacious method to model the intensity of moiré patterns. Denoting a moiré image as X, we first decompose it into sub-image patches as $\{x_i\}_{i=1}^{N}$. For a specific patch x, we use the Gaussian high-pass kernel (Dogra & Bhalla, 2014) to extract the frequency information as $\mathcal{F}(x)$. To measure the patch colorfulness, we consider a linear combination of the mean and standard deviation of the pixel cloud in the color plane of CIELab (Hasler & Suesstrunk, 2003):

$$\begin{aligned} C(x) = &\sqrt{\sigma^2(x_R - x_G) + \sigma^2(0.5(x_R + x_G) - x_B)} \\ &+0.3\sqrt{\mu^2(x_R - x_G) + \mu^2(0.5(x_R + x_G) - x_B)}, \end{aligned} \tag{1}$$

where $\mu(\cdot)$ and $\sigma(\cdot)$ are the mean and standard deviation functions, x_R, x_G, x_B denote the R, G, B color channels, respectively. Refer to (Hasler & Suesstrunk, 2003) for more principles of measuring image colorfulness. Therefore, our proposed moiré complexity score using frequency and colorfulness prior is finally defined as:

$$M(x) = C(x) \cdot \mu\big(F(x)\big). \tag{2}$$

Fig. 3 shows that $M(x)$ can be a reliable metric for evaluating the patch moiré complexity. Notice that, without building any extra network module, the operations of our moiré prior become highly cheap, bringing negligible computation burden.

3.2 Dynamic Demoiréing Acceleration

In image demoiréing, an moiré-polluted image X is expected to restore to moiré-free ground-truth in natural scenes. A traditional demoiréing process is formulated using CNNs as:

$$Y = \mathcal{F}(X; \Theta), \tag{3}$$

where $\mathcal{F}$ standards for the demoiréing network with its parameters denoted as Θ. As can be seen from Eq. (3), existing methods restore all areas of a moiré image with the same network $\mathcal{F}$, which

wastes excessive computation since the moiré complexity varies significantly across different areas of an image as aforementioned in Sec. 1. This violates our goal of real-time image demoiréing on mobile devices. A natural way for demoiréing acceleration is to reallocate computation costs according to the complexity of a moiré area.

To that effect, we reorganize the sub-image patches $\{x_i\}_{i=1}^{N}$ of X in an ascending order of their moiré complexity score defined in Eq. (2), and then split the ordered patches into M groups denoted as $\{G_1, G_2, ..., G_M\}$. Each group G_i contains these image patches, moiré complexity scores of which range from the top-$\big((i-1)\cdot\lceil\frac{N}{M}\rceil+1\big)$ to -$\big(i\cdot\lceil\frac{N}{M}\rceil\big)$ smallest among all. Then, we construct M different demoiréing networks $\{\mathcal{F}_i\}_{i=1}^{M}$ with parameters of different sizes as $\{\Theta_i\}_{i=1}^{M}$, and process each image patch $x \in G_i$ using the i-th network $\mathcal{F}_i$ as:

$$y = \mathcal{F}_i(x; \Theta_i | x \in G_i). \tag{4}$$

In our setting, the complexity of $\mathcal{F}_i$ is smaller than that of $\mathcal{F}_{i+1}$ such that smaller-complex image patches can be handled by networks with low computation costs , and vice versa. Eq. (4) dynamically accelerates the derivation of Eq. (3) by assigning computation costs in line with the degree of moiré complexity. Meanwhile, the recovery quality is still ensured as moiré centralized areas are restored using larger networks. Finally, the moiré-free output of our dynamic demoiréing acceleration method (DDA) is obtained by concatenating patch outputs of all networks:

$$Y = concat\big(\mathcal{F}_1(x; \Theta_1 | x \in G_1), \mathcal{F}_2(x; \Theta_2 | x \in G_2), ..., \mathcal{F}_M(x; \Theta_M | x \in G_M)\big), \tag{5}$$

where $concat()$ concatenates the output patches to construct a moiré-free full image.

3.3 Supernet Training

Though the aforesaid procedure benefits reduction of the overall computation costs, the challenge arises in respect of parameter burden when deploying our demoiréing method on mobile devices featured with short-supply memory. For a simple case, setting the largest network $\mathcal{F}_M$ as the vanilla demoiréing network $\mathcal{F}$, additional parameters of $\sum_{i=1}^{M-1}(|\Theta_i|)$ are introduced in total.

To solve this, in place of training networks $\{F_i\}_{i=1}^{M}$ in isolation, we further propose to use the supernet paradigm (Yang et al., 2021) to train and infer all networks in a parameter-shared manner. In details, the vanilla demoiréing network $\mathcal{F}$ is regarded as a supernet and its parameters Θ are partly shared by $\mathcal{F}_i$. Supposing the network width of $\mathcal{F}_i$ is W_i, we inherit the first W_i proportion of convolution filter weights to the subnet $\mathcal{F}_i$, denoted as $\Theta[W_i]$. Consequently, the network $\mathcal{F}_i$ becomes a subnet of $\mathcal{F}$. Therefore, our moiré-free output is finally reformulated as:

$$Y = concat\big(\mathcal{F}(x; \Theta[W_1] | x \in G_1), \mathcal{F}(x_2; \Theta[W_2] | x \in G_2), ..., \mathcal{F}(x; \Theta[W_M]) | x \in G_M\big). \tag{6}$$

As a consequence, image demoiréing can be effectively accelerated even without any additional parameter burden, which finally reaches our target for a real-time deployment on mobile devices.

4 Experiment

4.1 Experiment Setup

4.1.1 Datasets

There are three main public datasets for image demoiréing. (1) LCDMoiré dataset Yuan et al. (2019) from the AIM19 image demoiréing challenge consists of 10,200 synthetically generated image pairs including 10,000 training images, 100 validation images and 100 testing images at 1024×1024 resolution. (2) FHDMi dataset (He et al., 2020) contains 9981 image pairs for training and 2019 for testing with 1920×1080 resolution. (3) The TIP2018 dataset (Huang et al., 2017) consists of real photographs constructed by photographing images with 400×400 resolution from ImageNet (Deng et al., 2009) displayed on computer screens. In this paper, we conduct experiments on the LCDMoiré and FHDMi datasets. We do not consider the TIP2018 benchmark since the resolution is too small to meet our target for image demoiréing on mobile devices as the captured images generally have an extremely high-resolution with 1920×1080 or higher.

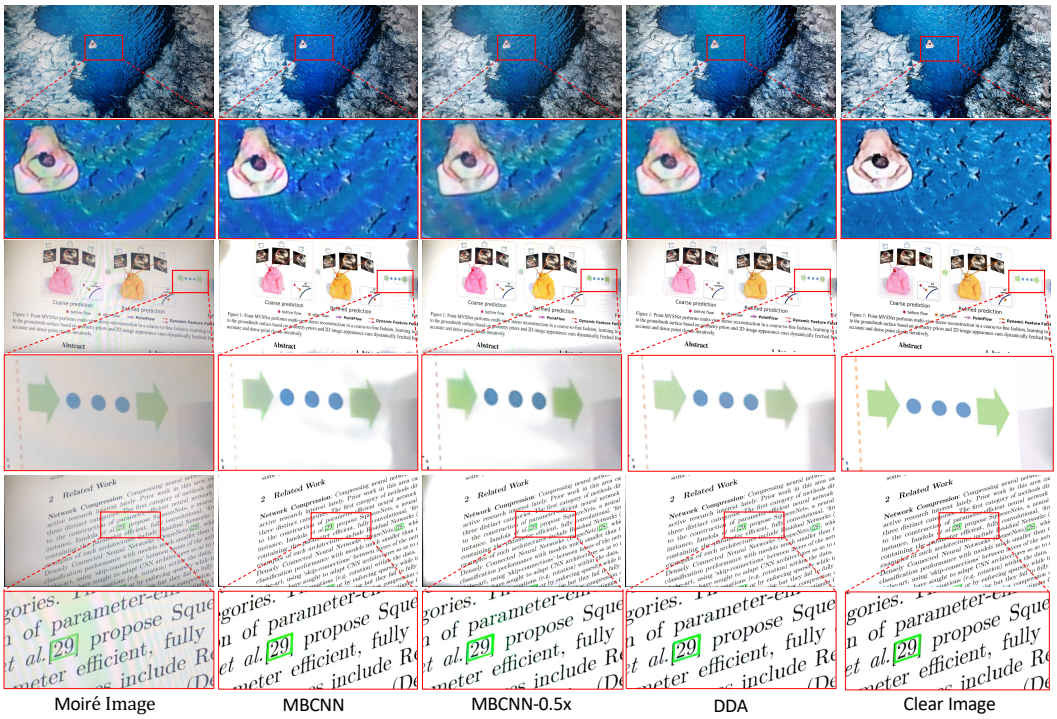

Figure 4: Visual quality comparison for accelerating MBCNN on the FHDMi dataset. The red boxes show a zooming-in area for better observation.

4.1.2 Evaluation Protocols

We adopt the widely-used metrics of PSNR (Peak Signal-to-Noise Ratio) and SSIM (Structure Similarity) to conduct a quantitative comparison for demoiréing performance. The Float Points Operations (denoted as FLOPs) and network latency per image on VIVO X80 Pro smartphone with the Snapdragon 8 Gen 1 chip of networks are reported as the accelerating evaluation.

4.1.3 Baselines

We choose to accelerate DMCNN (Huang et al., 2017) and MBCNN (Zheng et al., 2021) to verify the efficacy of our DDA method. DMCNN is a pioneer network for image demoiréing with multi-scale structure. MBCNN is a state-of-the-art demoiréing network, which consists of a learnable bandpass filter to learn the frequency prior and a two-step tone mapping mechanism to restore color information. We report the results of baseline models as well as their compact versions by slimming the network width.

4.1.4 Implement Details

Our implementation of DDA is based on the PyTorch framework (Paszke et al., 2019), with the group number $M = 3$, width list $W = \{0.25, 0.5, 0.75\}$ on FHDMI and $W = \{0.4, 0.5, 0.6\}$ on LCDMoiré. We split the original images of LCDMoiré and FHDMi datasets into sub-image patches of 512×512 and 640×540, respectively. We train the supernet using Adam (Kingma & Ba, 2014) optimizer. The initial learning rate and batch size are set to 1e-4 and 4 in all experiments. For DMCNN, we give 200 epochs for training with the learning rate divided by 10 at the 100-th epoch and 150-th epoch. For MBCNN, we follow (Zheng et al., 2021) to reduce the learning rate by half if the decrease in the validation loss is lower than 0.001 dB for four consecutive epochs and stop training once the learning rate becomes lower than 1e-6. All experiments are runned on NVIDIA Tesla V100 GPUs.

Table 1: Quantitative results for demoiréing acceleration on the FHDMi dataset.

Method	PSNR	SSIM	FLOPs	FLOPs ↓	Params	Params ↓	Latency
DMCNN	21.69	0.7731	699.16G	0.0%	1.43M	0.0%	69.4ms
DMCNN-0.75×	21.56	0.7704	476.62G	31.4%	0.99M	29.9%	55.2ms
DMCNN-0.5×	21.11	0.7691	314.82G	54.8%	0.68M	52.1%	47.9ms
DMCNN-0.25×	20.63	0.7655	208.73G	70.1%	0.48M	66.6%	41.8ms
DDA	**21.86**	**0.7708**	**333.39G**	**52.3%**	**0.99M**	**29.9%**	**48.0ms**
MBCNN	23.27	0.8201	4.22T	0.0%	14.21M	0.0%	259.8ms
MBCNN-0.75×	22.51	0.8113	3.05T	27.3%	11.88M	16.4%	192.4ms
MBCNN-0.5×	22.12	0.8077	2.07T	47.5%	9.92M	30.2%	147.2ms
MBCNN-0.25×	21.83	0.7991	1.28T	60.8%	8.36M	41.2%	119.7ms
DDA	**23.62**	**0.8293**	**2.13T**	**45.2%**	**11.88M**	**16.4%**	**147.1ms**

Table 2: Quantitative results for demoiréing acceleration on the LCDMoiré dataset.

Method	PSNR	SSIM	FLOPs	FLOPs ↓	Params	Params ↓	Latency
DMCNN	34.58	0.9612	353.11G	0.0%	1.43M	0.0%	35.2ms
DMCNN-0.75×	33.41	0.9589	242.24G	31.4%	0.99M	29.9%	28.0ms
DMCNN-0.5×	32.99	0.9604	159.67G	54.8%	0.68M	52.1%	24.2ms
DMCNN-0.25×	31.75	0.9547	105.42G	70.1%	0.48M	66.6%	21.1ms
DDA	**34.19**	**0.9601**	**158.71G**	**55.1%**	**0.78M**	**45.4%**	**24.4ms**
MBCNN	43.95	0.9909	2.14T	0.0%	14.21M	0.0%	132.1ms
MBCNN-0.75×	41.67	0.9853	1.55T	27.3%	11.88M	16.4%	98.1ms
MBCNN-0.5×	41.31	0.9844	1.05T	47.5%	9.92M	30.2%	76.3ms
MBCNN-0.25×	40.78	0.9801	0.65T	60.8%	8.36M	41.2%	61.2ms
DDA	**41.68**	**0.9869**	**1.09T**	**46.9%**	**10.61M**	**25.4%**	**75.2ms**

Table 3: Performance comparison between MBCNN accelerated by DDA and state-of-the-art demoiréing networks on the FHDMi dataset.

Method	DMCNN	MDNN	MopNet	FHDe^{2}Net	MBCNN	MBCNN-DDA
PSNR	21.69	20.83	22.76	22.93	23.14	**23.62**
SSIM	0.7731	0.7343	0.7958	0.7885	0.8201	**0.8293**
FLOPs	0.41T	0.47T	6.26T	11.41T	4.22T	**2.13T**
Params	2.37M	8.01M	12.4M	13.57M	14.99M	**10.61M**

4.2 Quantitative Comparison

Tab. 1 and Tab. 2 report the quantitative results of our DDA for accelerating DMCNN and MBCNN. On FHDMi, DDA surprisingly improves the PSNR of MBCNN by 0.35 dB even with a FLOPs reduction of 45.2%. We attribute such results to that the original baseline assigns the same network to restore the areas with little or no moiré patterns, which may damage the original details of the image. Consequently, the poor performance barricades the usage of demoiréing networks in practical deployment. In contrast, DDA leverage the smallest network to restore these non-moiré areas, leading to a better global demoiréing effect.

As to LCDMoiré, compared with DMCNN-0.75 which simply infers the whole image, our DDA dynamically assigns computation resources with respect to moiré complexity of patches, retaining a better PSNR performance (34.19 dB for DDA and 33.41 dB for DMCNN-0.75) and more FLOPs reduction (55.1% for DDA and 31.4% for DMCNN-0.75). Meanwhile, DDA achieves a noticeable latency reduction of 56.9 ms for accelerating MBCNN (75.2ms for DDA and 132.1ms for the baseline), enabling a real-time image demoiréing on mobile devices. These results well demonstrate the remarkable capability of DDA for accelerating demoiréing networks on the LCDemoiré dataset.

We further demonstrate the effectiveness of DDA by comparing MBCNN accelerated by it with several state-of-the-art demoiréing networks on FHDMi. As can be seen from Tab. 3, DDA can outperform other networks regarding both complexity reduction and demoiréing performance. For instance, DDA surpasses FHDe^{2}Net by 0.69 dB PSNR with even far fewer FLOPs (2.13 T for DDA and 11.41 T for FHDe^{2}Net), which shows the effectiveness of our perspective for reallocating computation costs in proportion to the complexity of moiré patches.

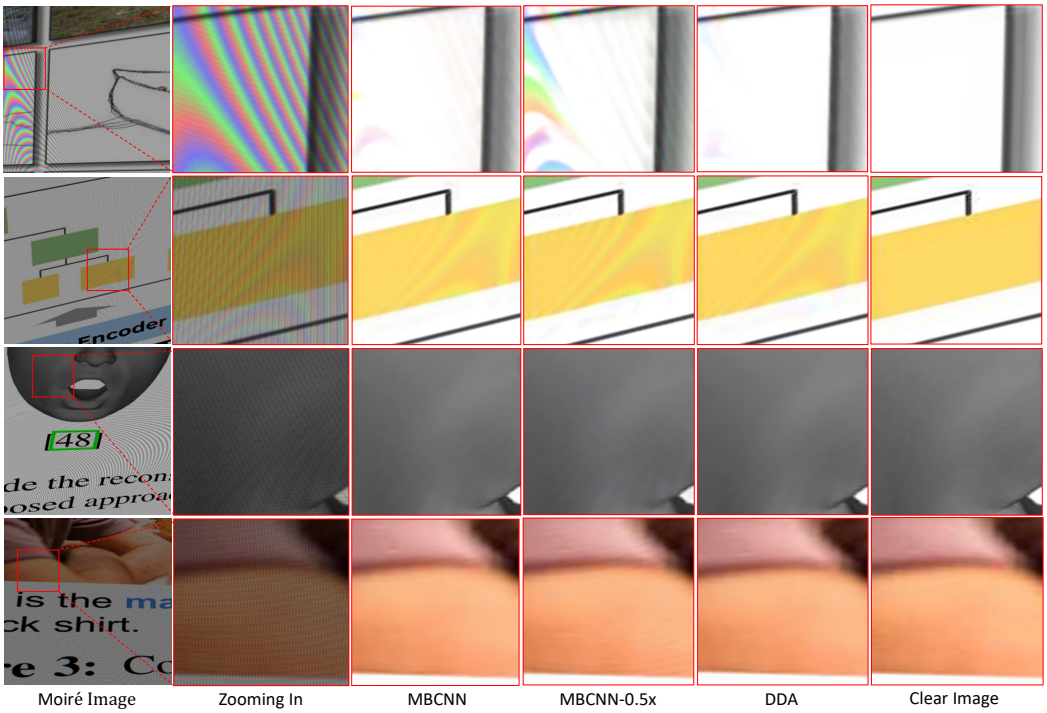

Figure 5: Visual quality comparison for accelerating MBCNN on the AIM19 dataset. The red boxes show a zooming-in area for better observation.

4.2.1 QUALITATIVE COMPARISON

In addition to the quantitative results, we further display the visualization of restored images in Fig. 4 and Fig. 5. As can be observed, uniformly performing the same accelerating rate for the whole image (MBCNN-0.5$\times$) drastically degrade the performance as the areas with dense moiré patterns do not receive enough computation resource to be efficiently restored. In contrast, by dynamically allocating the computational resources, our DDA achieves promising demoiréing quality compared with the original network. Thus, the efficacy of DDA for accelerating demoiréing networks for practical application is well demonstrated.

4.3 PERFORMANCE ANALYSIS

In this section, we perform detailed performance anon the different components of our DDA including the supernet training paradigm and moiré prior.

4.3.1 SUPERNET TRAINING

We first conduct experiments to investigate how the hyper-parameters in the supernet training influence the performance of DDA, *w.r.t*, the width list configuration W. The experiments are conducted on the FHDMi dataset using MBCNN. We can observe from Tab. 4 that a dispersed configuration $W = \{0.25, 0.5, 0.75\}$ performs better on the FHDMi dataset, while a compact configuration $W = \{0.4, 0.5, 0.6\}$ works better on the AIM19 dataset. To explain, AIM19 is a synthetic dataset, where the moiré patterns distribute more balanced compared with FHDMi that is captured using embedded cameras. Self-confidently, a more discrete width list guarantees our purpose of dynamically removing moiré patches of different complexity in real scenarios.

Besides, Tab. 5 compares the performance for accelerating MBCNN on LCDMoire between supernet training and respectively training each sub-network. It can be seen that supernet training does not lead to performance degradation and it drastically reduces the parameter burden compared with

simultaneously keeping multiple sub-networks, which demonstrates the effectiveness of our DDA for practical deployment.

Table 4: Ablation study of DDA for applying different width list configuration in supernet training.

	FHDMi			AIM		
W	PSNR	SSIM	Params	PSNR	SSIM	Params
$\{0.4, 0.5, 0.6\}$	22.81	0.8124	10.61M	41.68	0.9869	10.61M
$\{0.25, 0.5, 0.75\}$	23.07	0.8766	11.88M	41.43	0.9852	11.88M
$\{0.1, 0.5, 0.9\}$	21.03	0.7988	13.15M	40.21	0.9791	13.15M

Table 5: Ablation study of DDA for dynamic acceleration with/without supernet training.

Method	PSNR	Params
w supernet	23.62	11.88M
w/o supernet	23.15	30.16M

Table 6: Ablation study of DDA for restoring each patch group with different widths.

Network	G_1	G_2	G_3
MBCNN-0.75×	24.03	22.21	21.29
MBCNN-0.5×	24.12	22.02	20.22
MBCNN-0.25×	23.99	21.81	19.69

Table 7: Ablation study of DDA for components in the moiré prior.

Prior	PSNR
C	22.44
F	22.18
CF (DDA)	23.62

4.3.2 MOIRÉ PRIOR

We further analyze the performance of the proposed moiré prior. The experiments are conducted on the FHDMi dataset using MBCNN. We use networks of different widths to infer different groups of pictures with different complexity classified by our proposed moiré prior. The results for Tab. 6 show that all widths perform similarly for the easiest group, while larger width significant outperforms smaller width for the group with highest moiré complexity. Such results demonstrate the effectiveness of our proposed moiré prior operator, and also validate our point that using large networks to restore patches with low moiré complexity wastes massive computation resources.

At last, we compare two variants for only using high-frequency information (denoted as F) or colorfulness information (denoted as C) with the proposed moiré prior that considers both (denoted as CF). As shown in Tab.7, both these two variants result in worse performance, which well demonstrates the efficacy of our proposed moiré prior that considers both color and frequency properties of moiré patterns. Thus, our prior offers reliable moiré complexity for a given image patch.

5 LIMITATION AND FUTURE WORK

We further discuss the limitations of our DDA, which will be our future focus. Firstly, DDA simply divides all images into equal-number patches in each class, laying some avenues for future research in devising image-aware classification priors. Besides, our limited computing facilities prevent us from accelerating other demoiréing networks with varying structures (Liu et al., 2020; He et al., 2019). More validations are expected to be performed to further demonstrate the efficacy of DDA.

6 CONCLUSION

In this paper, we present a novel dynamic demoiréing acceleration method (DDA) to reduce the huge computational burden of existing networks towards real-time demoiréing on mobile devices. Our DDA is based on the observation that the moiré complexity is highly unbalanced across different areas of an image. On this basis, we propose to split the whole image into sub-patches, which are then regrouped according to their moiré complexities measured by a novel moiré prior that considers both the frequency and colorfulness information. Then, we use models with different sizes to restore patches in each group. In particular, larger networks are utilized to restore moiré centralized areas to ensure the recovery quality while smaller networks are leveraged to restore moiré diluted areas to relieve computation burden. To avoid the additional parameter burden caused by retaining multiple networks, we further leverage the supernet paradigm to jointly train the networks in a parameter-shared manner. Results on several benchmarks demonstrate that our method can effectively reduce the computation costs of existing networks with negligible performance degradation, enabling a real-time demoiréing on nowadays smartphones.

REFERENCES

Tolga Bolukbasi, Joseph Wang, Ofer Dekel, and Venkatesh Saligrama. Adaptive neural networks for efficient inference. In *International Conference on Machine Learning (ICML)*, pp. 527–536. PMLR, 2017.

Bohong Chen, Mingbao Lin, Kekai Sheng, Mengdan Zhang, Peixian Chen, Ke Li, Liujuan Cao, and Rongrong Ji. Arm: Any-time super-resolution method. In *European Conference on Computer Vision (ECCV)*, 2022.

Jia Deng, Wei Dong, Richard Socher, Li-Jia Li, Kai Li, and Li Fei-Fei. Imagenet: A large-scale hierarchical image database. In *IEEE Conference on Computer Vision and Pattern Recognition (CVPR)*, pp. 248–255, 2009.

Ayush Dogra and Parvinder Bhalla. Image sharpening by gaussian and butterworth high pass filter. *Biomedical and pharmacology journal*, 7(2):707–713, 2014.

Yizeng Han, Gao Huang, Shiji Song, Le Yang, Honghui Wang, and Yulin Wang. Dynamic neural networks: A survey. *IEEE Transactions on Pattern Analysis and Machine Intelligence (TPAMI)*, 2021.

David Hasler and Sabine E Suesstrunk. Measuring colorfulness in natural images. In *Human vision and electronic imaging VIII*, volume 5007, pp. 87–95. International Society for Optics and Photonics, 2003.

Bin He, Ce Wang, Boxin Shi, and Ling-Yu Duan. Mop moire patterns using mopnet. In *Proceedings of the IEEE/CVF International Conference on Computer Vision (ICCV)*, pp. 2424–2432, 2019.

Bin He, Ce Wang, Boxin Shi, and Ling-Yu Duan. Fhde 2 net: Full high definition demoireing network. In *European Conference on Computer Vision (ECCV)*, pp. 713–729. Springer, 2020.

Gao Huang, Danlu Chen, Tianhong Li, Felix Wu, Laurens Van Der Maaten, and Kilian Q Weinberger. Multi-scale dense networks for resource efficient image classification. In *Advances in Neural Information Processing Systems (NeurIPS)*, 2017.

Diederik P Kingma and Jimmy Ba. Adam: A method for stochastic optimization. *arXiv preprint arXiv:1412.6980*, 2014.

Xiangtao Kong, Hengyuan Zhao, Yu Qiao, and Chao Dong. Classsr: A general framework to accelerate super-resolution networks by data characteristic. In *Proceedings of the IEEE/CVF Conference on Computer Vision and Pattern Recognition (CVPR)*, pp. 12016–12025, 2021.

Fanglei Liu, Jingyu Yang, and Huanjing Yue. Moiré pattern removal from texture images via low-rank and sparse matrix decomposition. In *2015 Visual Communications and Image Processing (VCIP)*, pp. 1–4. IEEE, 2015.

Lin Liu, Jianzhuang Liu, Shanxin Yuan, Gregory Slabaugh, Aleš Leonardis, Wengang Zhou, and Qi Tian. Wavelet-based dual-branch network for image demoiréing. In *European Conference on Computer Vision (ECCV)*, pp. 86–102. Springer, 2020.

Adam Paszke, Sam Gross, Francisco Massa, Adam Lerer, James Bradbury, Gregory Chanan, Trevor Killeen, Zeming Lin, Natalia Gimelshein, Luca Antiga, et al. Pytorch: An imperative style, high-performance deep learning library. In *Advances in Neural Information Processing Systems (NeurIPS)*, pp. 8026–8037, 2019.

Yujing Sun, Yizhou Yu, and Wenping Wang. Moiré photo restoration using multiresolution convolutional neural networks. *IEEE Transactions on Image Processing (TIP)*, 27(8):4160–4172, 2018.

Jingyu Yang, Fanglei Liu, Huanjing Yue, Xiaomei Fu, Chunping Hou, and Feng Wu. Textured image demoiréing via signal decomposition and guided filtering. *IEEE Transactions on Image Processing (TIP)*, 26(7):3528–3541, 2017a.

Jingyu Yang, Xue Zhang, Changrui Cai, and Kun Li. Demoiréing for screen-shot images with multi-channel layer decomposition. In *2017 IEEE Visual Communications and Image Processing (VCIP)*, pp. 1–4. IEEE, 2017b.

Taojiannan Yang, Sijie Zhu, Matias Mendieta, Pu Wang, Ravikumar Balakrishnan, Minwoo Lee, Tao Han, Mubarak Shah, and Chen Chen. Mutualnet: Adaptive convnet via mutual learning from different model configurations. *IEEE Transactions on Pattern Analysis and Machine Intelligence (TPAMI)*, 2021.

Jiahui Yu and Thomas S Huang. Universally slimmable networks and improved training techniques. In *Proceedings of the IEEE/CVF International Conference on Computer Vision (ICCV)*, pp. 1803–1811, 2019.

Shanxin Yuan, Radu Timofte, Gregory Slabaugh, and Aleš Leonardis. Aim 2019 challenge on image demoireing: Dataset and study. In *2019 IEEE/CVF International Conference on Computer Vision Workshop (ICCVW)*, pp. 3526–3533. IEEE, 2019.

Bolun Zheng, Shanxin Yuan, Gregory Slabaugh, and Ales Leonardis. Image demoireing with learnable bandpass filters. In *Proceedings of the IEEE/CVF Conference on Computer Vision and Pattern Recognition (CVPR)*, pp. 3636–3645, 2020.

Bolun Zheng, Shanxin Yuan, Chenggang Yan, Xiang Tian, Jiyong Zhang, Yaoqi Sun, Lin Liu, Ales Leonardis, and Greg Slabaugh. Learning frequency domain priors for image demoireing. *IEEE Transactions on Pattern Analysis and Machine Intelligence (TPAMI)*, 2021.